

# Electrooptic despeckler based on helix-free ferroelectric liquid crystal

A.L. Andreev, N.V. Zalyapin, T.B. Andreeva, I.N. Kompanets

**Abstract.** In an experimental sample of a despeckler, consisting of an electrooptic cell with a 20- $\mu\text{m}$ -thick helix-free liquid ferroelectric, to which an electric field with a strength of  $\sim 3\text{V } \mu\text{m}^{-1}$  and a frequency of 2 kHz is applied, we obtained spatially nonuniform phase modulation of a laser beam with a value exceeding  $\pi$ . The effect allows the implementation of speckle noise suppression with an efficiency of 10.7 dB.

**Keywords:** holography, speckle noise, despeckler, liquid crystal, light scattering, phase modulation of light, beam coherence destruction, speckle suppression.

## 1. Introduction

The authors of Refs [1, 2] proposed a method of speckle noise suppression in laser images using a simple optical modulator, namely, an electrooptic cell, in which a ferroelectric liquid crystal (FLC) having a spiral (helicoidal) structure was used. The phasing of waves in a laser beam and, therefore, their ability to interfere, giving rise to speckle noise, was destructed in real time, when the laser beam passed the FLC, to which a sequence of two-frequency bipolar electric pulses of special shape was applied. This results in the formation of small-scale patterns in the volume of the FLC with a random distribution of refractive index gradients rapidly varying in time. The resulting chaotic modulation of the position of the FLC scattering indicatrix finally caused the phase modulation, spatially nonuniform in the cell aperture, with a value of the order of  $\pi$  and greater.

The advantages of using a FLC cell as a despeckler are obvious [2, 3]:

(i) in comparison with mechanical devices (vibrating membrane or rotating phase mask) a FLC-based despeckler provides simplicity, stability and long-term reliable operation;

(ii) in comparison with a phase spatial modulator, forming orthogonal functions (in fact, a microdisplay), the construction, technology and control electronics are essentially simplified;

(iii) in comparison with a photopolymer medium, in which multiple speckle patterns are recorded in the form of overlap-

ping holograms, critical changes in wavelength, noise and ‘tiredness’ are absent in a FLC despeckler; and

(iv) in comparison with a light-scattering diffusor, with a reliefographic modulator of light implemented using a reflecting diffraction grating, with the devices of beam scanning and mixing in fibre waveguides and tubes, as well as with the devices using lasers with frequency doubling and parametric oscillation, a FLC despeckler is essentially more compact and provides smaller light losses.

It is also important that the well-developed technology allows variation of the FLC despeckler aperture size from parts of a square centimetre to a few square centimetres, its thickness being 1–2 mm, including the control chip.

It is worth noting that the modulation frequency of the light radiation in the regime of spatially nonuniform phase modulation in the electrooptic cell with a helicoidal FLC did not exceed 400 Hz and was independent of the electric field strength at  $E \geq 2 \text{ V } \mu\text{m}^{-1}$  [3], which obviously limited the field of possible applications of the despeckler. Further use of the electrooptic cell with a helix-free FLC allowed the phase delay modulation frequency to be increased to 1 kHz [4, 5]. The helicoidal twist of the director (the direction of the main optical axis of the FLC) was suppressed at the expense of the interaction of chiral additions with opposite signs of optical activity. The spatially nonuniform phase modulation of light in the volume of a helix-free FLC and the suppression of speckle noise in the images formed by the laser was achieved under the simultaneous impact of the high-frequency (up to 10kHz) and low-frequency (up to 1000 Hz) pulsed voltage. The main advantages of the modulator, alongside with an increase in the frequency of phase delay modulation, are the absence of distortion in the spectral composition of the modulated light and the absence of light scattering, when the electric field is switched off, caused by the suppression of the helicoid. Besides that, the similar shape of the pulses of the low-frequency and high-frequency voltage allowed the electronic control circuit of the modulator to be simplified.

Considering the progress achieved in the usage of a helix-free FLC in the electrooptic despeckler, we carried out the work aimed at the optimisation of the FLC and the regime of electric control. Along with this, the technique of speckle pattern image recording and processing by means of special mathematical and software tools was mastered.

## 2. Technique of speckle pattern recoding and processing

As in most papers related to speckle recording and suppression, we use the following technique. A laser beam passed through a speckle-suppressing device (despeckler) is directed to a CCD camera that records the intensity distribution in the

A.L. Andreev, N.V. Zalyapin, T.B. Andreeva P.N. Lebedev Physical Institute, Russian Academy of Sciences, Leninsky prosp. 53, 119991 Moscow, Russia;

I.N. Kompanets P.N. Lebedev Physical Institute, Russian Academy of Sciences, Leninsky prosp. 53, 119991 Moscow, Russia; National Research Nuclear University ‘MEPhI’, Kashirskoye sh. 31, 115409 Moscow, Russia; e-mail: kompan@sci.lebedev.ru

Received 16 August 2017

*Kvantovaya Elektronika* 47 (11) 1064–1068 (2017)

Translated by V.L. Derbov

beam cross section in the absence of the control voltage at the electrodes of the FLC cell (before the suppression of speckles) and in the presence of the control voltage (when the speckles are to some extent suppressed).

Obtained images of speckle patterns were processed using specially elaborated software calculating speckle pattern parameters (intensity, contrast ratio, attenuation coefficient) to plot the profiles of the intensity distribution in the laser spot image. The software incorporated the Python Image Library (PIL) for operating with raster graphics and images [6] that comprised the basic functions of image processing, including the possibility to obtain the numerical values of colours ( $R$ ,  $G$ ,  $B$ ) of a pixel using the method `getpixel(i, j)`, where  $i$  and  $j$  are the pixel coordinates in the image. From the values of  $R$ ,  $G$ , and  $B$  the values of intensity were calculated. The obtained data (the coordinates of pixels and the corresponding values of intensity) were loaded into the MS Excel file, created by the programme. To solve this task, we used the `xlwt` library that allowed the creation and filling of Excel files.

To calculate the contrast of speckle patterns we used the relation [7]:

$$C = \sigma/\langle I \rangle, \quad (1)$$

where  $\sigma$  is the root-mean-square deviation of the intensity fluctuation, and  $\langle I \rangle$  is the mean value of the intensity. The contrast ratio  $C$  of the speckle pattern varies from 0 to 1. The maximal possible value  $C = 1$  is achieved only in the speckle patterns observed in the case of broad laser beams diffracted on a strongly rough surface or strongly scattering transparency.

The lower limit of intensity (0) determines the level of black in the speckle pattern image and the upper limit (255) corresponds to the level of white. The intermediate intensity values fill the dynamic range forming halftones in the image, i.e., the grey scale that characterises the light intensity at each pixel of the recording CCD matrix.

The efficiency of reducing the speckle pattern contrast was calculated as the ratio (in decibels) of the contrast ratio with the despeckler switched off ( $C_1$ ) and that with the despeckler switched on ( $C_n$ ) [8]:

$$R = 10\lg(C_1/C_n). \quad (2)$$

### 3. Experimental results

In the work we used a helix-free FLC with the following parameters: spontaneous polarisation,  $P_s = 40 \text{ nC cm}^{-2}$ ; rotation viscosity coefficient,  $\gamma_\phi = 0.7$  poise; tilt angle of the molecules in smectic layers,  $\Theta_0 = 23^\circ$  (at a temperature of  $20^\circ\text{C}$ ); and temperature interval of ferroelectric phase existence, from  $2^\circ\text{C}$  to  $75^\circ\text{C}$ .

In the electrooptic cell with the helix-free FLC the light is scattered at the boundaries of spontaneously ordered domains formed due to the appearance of waves with a stationary profile, i.e., the dynamic solitons [9]. The dynamic solitons arise in the structure with periodic deformations of smectic layers that lead to periodic changes in the director position along each layer with the transition to the Maxwellian energy dissipation mechanism in the nonlinear process of the FLC director reorientation in the alternating electric field. The smectic layers are treated as periodic ordering of the molecular centres of mass along the director

with a period of the order of the FLC molecule length. For the used FLC, the period of layer deformation lies within the limits  $1.5\text{--}2 \mu\text{m}$ .

The alternating electric field applied along the smectic layers and interacting with the spontaneous polarisation changes the director distribution in each of the layers. The development of this process leads to the appearance of solitons, which are wave packets with a periodic wave localised in them [9]. In turn, they cause the appearance of the refractive index gradients, i.e. the centres of light scattering (transient domains), and the light transmission and the scattering efficiency (contrast ratio) depend on the frequency of the electric field change.

The maximal light scattering efficiency corresponds to the regular structure of scattering centres in the form of circular domains having a sufficiently uniform distribution over the FLC volume. Depending on the frequency of the electric field variation or the duration of the control voltage pulses and the thickness of the electrooptic cell, one can observe several maxima of the light scattering efficiency, or the light scattering modes [9].

The transitions between the light scattering modes, to which the maxima of the light scattering efficiency correspond, result in the chaotic changes in the scattering indicatrix position and in the spatially nonuniform modulation of the phase delay, when voltage pulses with a duration corresponding to different maxima are simultaneously applied to the electrooptic cell, [4, 9].

As a result of short-time (less than  $30 \mu\text{s}$ ) switching on of the light scattering in the FLC volume, the patterns with a random distribution of the refractive index gradient are formed, which, in turn, cause the phase modulation of light in the electrooptic cell, spatially nonuniform in the beam cross section. Note that the eyes are not sensitive to such short-time light scattering, and so it does not distort the structure of images and does not affect their perception, and the light losses here are insignificant (less than 5%).

In the absence of the control voltage applied to the electrooptic cell, the contrast ratio of the speckle pattern for a semiconductor laser with the wavelength  $\lambda = 0.65 \mu\text{m}$  amounts to 0.82 (Fig. 1).

The amplitude, the duration, the repetition rate of the low-frequency and high-frequency voltage pulses and the modulation depth were chosen to provide the phase delay modulation with a maximal degree of inhomogeneity and to attain a maximal possible frequency of the spatially nonuniform phase modulation under the condition that the efficiency of the light scattering varies during the action of each pulse of the sequence, but does not reach its maximal value.

For electrooptic cells having the thickness within the limits  $8\text{--}13 \mu\text{m}$ , only one maximum of the light scattering efficiency was observed. In this case, the light transmission and the light scattering efficiency depend only on the frequency of electric field variation. Besides that, there are only two light scattering modes, the low-frequency mode and the high-frequency one. In the low-frequency mode (having a frequency lower than  $200 \text{ Hz}$ ), the transition to the scattering state occurs at each change of the electric fields sign, and the efficiency of light scattering is independent of the voltage polarity. In the high-frequency mode (having a frequency higher than  $1 \text{ kHz}$ ), the light scattering efficiency depends on the polarity of the control voltage and the duration of the scattering process increases with increasing frequency.

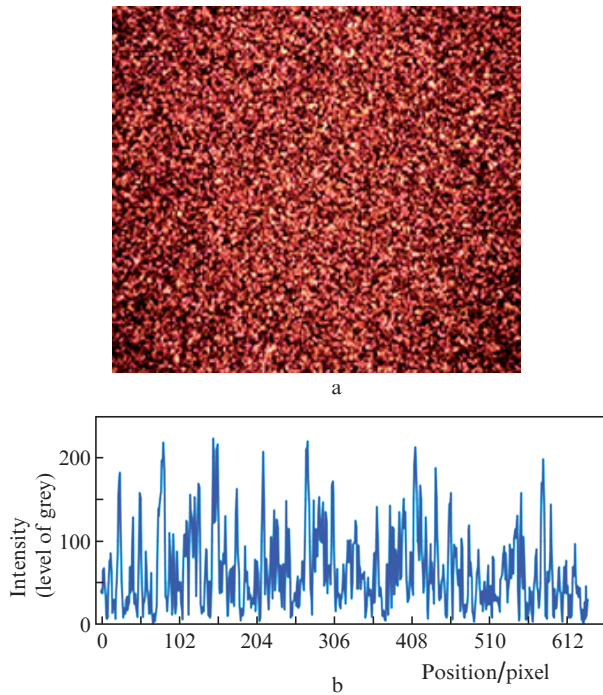


**Figure 1.** (a) Photograph of the intensity distribution of radiation in the cross section of the laser beam passed through the electrooptic cell in the absence of the control voltage and (b) intensity distribution at the analysed pixels along the horizontal line in the centre of the photograph; the electrooptic cell thickness is  $13\ \mu\text{m}$ ,  $C_1 = 0.82$ ,  $\lambda = 0.65\ \mu\text{m}$ .

The phase delay modulation with a high degree of nonuniformity was observed, e.g., in modulating the high-frequency voltage (meander) with a signal having different durations of the leading and trailing pulse edges, in particular, with a saw-shaped voltage (Fig. 2). When we applied such a voltage to the electrooptic cell, the contrast ratio of the speckle pattern decreased to 0.1 (Fig. 3). The efficiency of speckle noise sup-

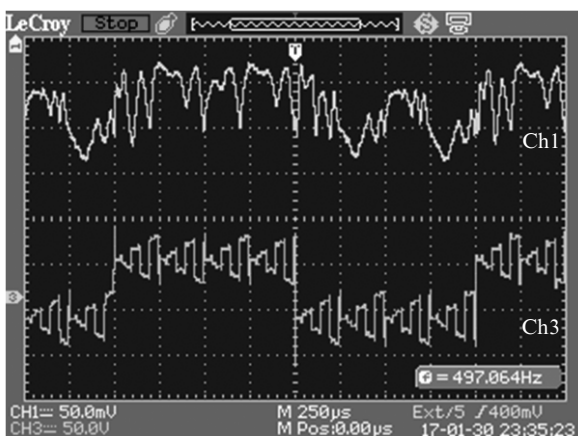


**Figure 2.** Oscillograms of the control voltage (channel Ch3) and phase delay modulation (channel Ch1). The repetition rate of the low-frequency signal (meander) is 500 Hz, the amplitude is  $\pm 32\ \text{V}$ , the frequency of the modulating signal is 10 kHz (meander modulated by a triangle-shaped signal with the frequency 4 kHz), the amplitude of the modulating signal varies from 0 to  $\pm 13\ \text{V}$ , the thickness of the electrooptic cell is  $13\ \mu\text{m}$ , the electric field strength  $E = 3.46\ \text{V}\ \mu\text{m}^{-1}$ .

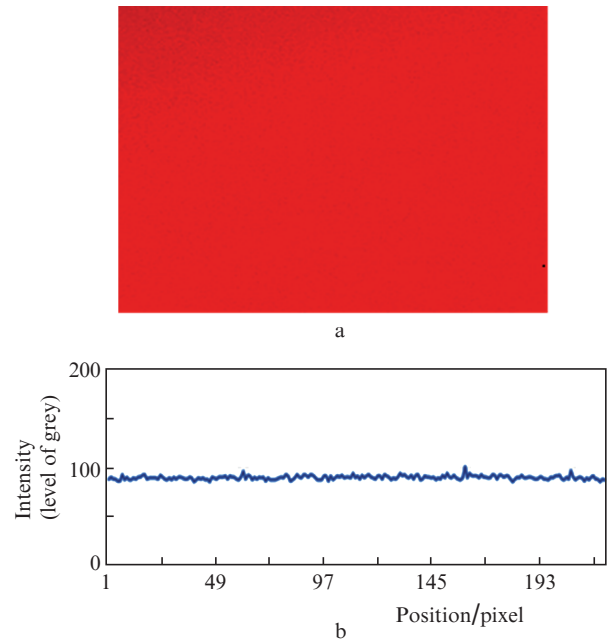


**Figure 3.** (a) Photograph of the radiation intensity distribution in the cross section of the laser beam passed through the electrooptic cell with the applied control voltage, and (b) intensity distribution at the analysed pixels along the horizontal line in the centre of the photograph; the electrooptic cell thickness is  $13\ \mu\text{m}$ ,  $C_2 = 0.1$ ,  $\lambda = 0.65\ \mu\text{m}$ .

pression, understood as a decrease in the contrast ratio of the speckle patterns in Fig. 1 (between the contrast ratios  $C_1$  and  $C_2$ ), amounted to 9.1 dB.

Note that the frequency of the spatially nonuniform phase modulation in the electrooptic cell  $13\ \mu\text{m}$  thick does not exceed 500 Hz, because the interval in which the low-frequency mode exists is limited by the control voltage frequency ( $\sim 200\ \text{Hz}$ ), and the transition to the high-frequency mode begins at a frequency  $\sim 700\ \text{Hz}$ . The transition frequency decreases with decreasing electric field strength and becomes independent of the field strength at  $E \geq 3\ \text{V}\ \mu\text{m}^{-1}$ .

As mentioned above, for electrooptic cells having a thickness between 8 and  $13\ \mu\text{m}$ , only one maximum of light scattering efficiency was observed. The second maximum appears when the thickness of the cell is increased to  $15\text{--}17\ \mu\text{m}$ . In this case, the transitions between the light scattering modes, to which the light scattering efficiency maxima correspond, lead to a chaotic variation in the scattering indicatrix position, when bipolar voltage pulses having a duration corresponding to different maxima are applied to the electrooptic cell.

As a result, the phase modulation with a high degree of nonuniformity was achieved under the amplitude modulation of the low-frequency control voltage (meander with a frequency 1 kHz) with a high-frequency voltage of the same shape with a frequency 5 kHz, the electric field strength being  $\sim 3.5\ \text{V}\ \mu\text{m}^{-1}$  (Fig. 4). When, as in the previous case, the control voltage was applied to the electrooptic cell, the contrast ratio of the speckle pattern decreased to 0.1, but the frequency of phase delay modulation increased to 1 kHz at the same electric field strength, as for the cell  $13\ \mu\text{m}$  thick. The efficiency of speckle noise suppression amounted to 9.1 dB. Note that in this case an increase in the frequency of both low-frequency and high-



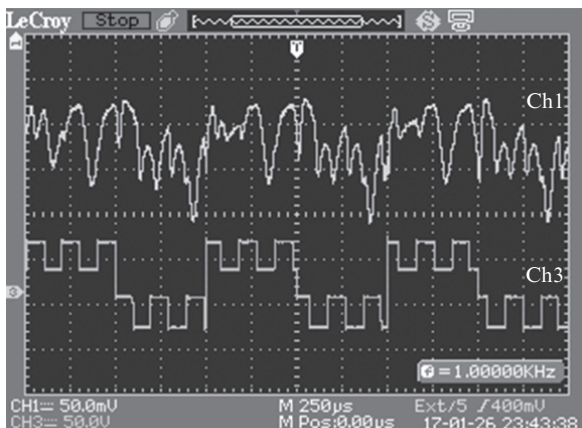


**Figure 4.** Oscillograms of the control voltage (channel Ch3) and phase delay modulation (channel Ch1). The repetition rate of the low-frequency signal (meander) is 1 kHz, the amplitude is  $\pm 40$  V, the frequency of the modulating signal (meander) is 5 kHz, the amplitude is  $\pm 15$  V, the thickness of the electrooptic cell is  $16 \mu\text{m}$ ,  $E = 3.44 \text{ V } \mu\text{m}^{-1}$ .

frequency voltage above 1 and 5 kHz, respectively, at the unchanged electric field strength leads to the growth of the speckle pattern contrast.

The third maximum of the light scattering efficiency appeared when the thickness of the electrooptic cell increased to  $18 \mu\text{m}$  [3, 9]. For the cell thickness  $20 \mu\text{m}$  and more, the maxima begin to shift towards shorter pulses of the control voltage, which allows the phase delay modulation frequency to be increased without increasing the electric field strength. Thus, for the cell  $\sim 20 \mu\text{m}$  thick at the electric field strength  $3.25 \text{ V } \mu\text{m}^{-1}$  the phase modulation with a high degree of non-uniformity was achieved under the amplitude modulation of the low-frequency bipolar voltage (meander) having the frequency 2 kHz with the high-frequency signal of the same shape and frequency 7 kHz (Fig. 5).

The phase delay modulation by a low-frequency and high-frequency control voltage and the simultaneous application of the voltage pulses with a duration corresponding to the

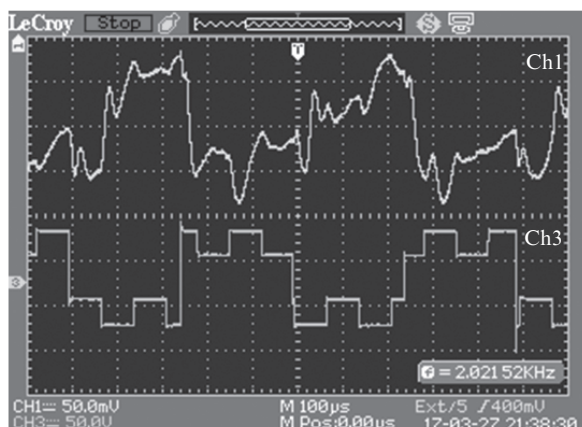


**Figure 5.** Oscillograms of the control voltage (channel Ch3) and phase delay modulation (channel Ch1). The repetition rate of the low-frequency signal (meander) is 2 kHz, the amplitude is  $\pm 50$  V, the frequency of the modulating signal (meander) is 7 kHz, the amplitude is  $\pm 15$  V, the thickness of the electrooptic cell is  $20 \mu\text{m}$ ,  $E = 3.25 \text{ V } \mu\text{m}^{-1}$ .

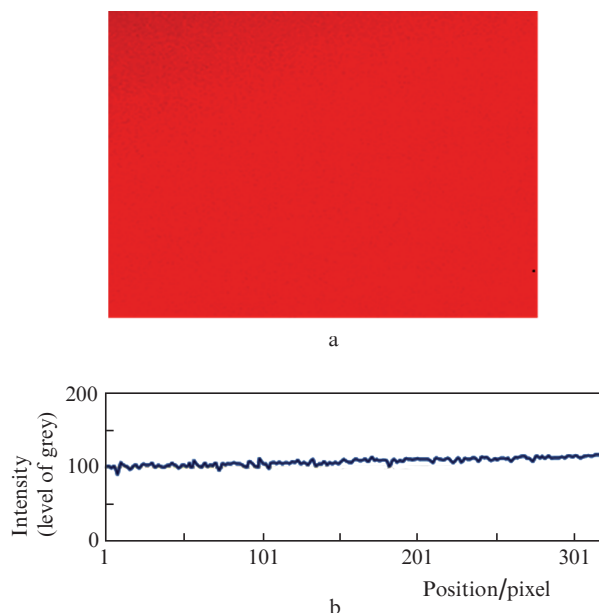


**Figure 6.** (a) Photograph of the radiation intensity distribution in the cross section of the laser beam passed through the electrooptic cell with the control voltage applied to it, and (b) intensity distribution at the analysed pixels (along the horizontal line in the centre of the photograph);  $C_3 = 0.07$ , the electrooptic cell thickness is  $20 \mu\text{m}$ ,  $\lambda = 0.65 \mu\text{m}$ .

first and the second maximum of the light scattering efficiency provided the reduction of the contrast ratio in the speckle pattern to 0.07 (Fig. 6). The efficiency of reducing the contrast ratio of the speckle pattern amounted to 10.7 dB, and the frequency of phase delay modulation increased to 2 kHz, the electric field strength being smaller than for the cells 13 and  $16 \mu\text{m}$  thick.

#### 4. Conclusions

In the case of short-term (less than  $30 \mu\text{s}$ ) switching on of light scattering in the volume of a helix-free FLC, the patterns with a random distribution of refractive index gradients are formed, which, in turn, cause the phase modulation of light in the electrooptic cell, spatially nonuniform in the cross section of the beam. In the presence of the electric field having a strength about  $3 \text{ V } \mu\text{m}^{-1}$ , this modulation having a value of the order of  $\pi$  and greater made it possible to efficiently suppress speckle noise in the laser beam cross section. The efficiency of contrast reduction in the speckle pattern amounted to 10.7 for the phase delay modulation frequency of 2 kHz without distortions in the spectral composition of the modulated radiation.

Depending on technical requirements, the electrooptic despeckler based on a helix-free FLC can operate at sufficiently small (to 35 V) control voltages if the electrooptic cell thickness is within the limits  $10\text{--}13 \mu\text{m}$ . In this case, the reduction of contrast of the speckle pattern amounts to about 9 dB, but the frequency of phase delay modulation does not exceed 500 Hz. On the other hand, an increase in the cell thickness to  $18\text{--}20 \mu\text{m}$  allows the speckle pattern contrast to be reduced by 10.7 dB and the frequency of phase delay modulation to be increased to 2 kHz. However, the amplitude of the control voltage in this case increases to  $60\text{--}65 \text{ V}$ .

**Acknowledgements.** The work was supported by the Presidium of the Russian Academy of Sciences ('Fundamental and Applied Problems of Photonics and Physics of New Optical Materials' Programme No. 25) and by the Programme for Increasing Competitiveness of the National Research Nuclear University 'MEPhI'.

## References

1. Andreev A.L., Kompanets I.N., Minchenko M.V., Pozhidaev E.P., Andreeva T.B. *Quantum Electron.*, **38** (12), 1166 (2008) [*Kvantovaya Elektron.*, **38** (12), 1166 (2008)].
2. Kompanets I.N., Andreev A.L. Patent of Russian Federation No. 2373558 (2009).
3. Andreev A.L., Andreeva T.B., Kompanets I.N., Minchenko M.V., Pozhidaev E.P. *J. of SID*, **17**, 801 (2009).
4. Andreev A.L., Andreeva T.B., Kompanets I.N., Zalyapin N.V. *Quantum Electron.*, **44** (12), 1136 (2014) [*Kvantovaya Elektron.*, **44** (12), 1136 (2014)].
5. Kompanets I.N., Andreev A.L., Andreeva T.B. Patent of Russian Federation No. 561307 (2015).
6. Python Image Library. URL: <http://www.pythonware.com/products/pil/>; <http://effbot.org/imagingbook/>; <http://www.python-excel.org/>.
7. Goodman J.W. *J. Opt. Soc. Am.*, **66**, 1145 (1976).
8. *LSR-3000 & LSR-OEM Series. Laser Speckle Reducer (Application Note)*. Update: 07.07.2011.
9. Andreev A., Andreeva T., Kompanets I., Zalyapin N., Xu H., Pivnenko M., Chu D. *Appl. Opt.*, **55**, 3483 (2016).